MATEC Web of Conferences **5**, 04037 (2013)
DOI: 10.1051/matecconf/20130504037

First-principles study of structural and electronic properties of Laves phases structures YM_2 (M = Cu and Zn)

M.K. Benabadji and H.I. Faraoun

Laboratory of Study and Discovery of Materials, Unit of Research Materials and Renewable Energy, University of Tlemcen, Algeria

Abstract. First-principles calculations have been carried out to investigate the structural properties and electronic structure of the main binary Laves phase YCu_2 and YZn_2 with C14, C14, C36 and $CeCu_2$ structures in Cu-Y-Zn alloy, respectively. The total energies of Laves phases with various occupations of nonequivalent lattice sites in all four structural forms have been calculated Ab initio by a pseudopotential VASP code. The optimized structural parameters were in very good agreement with the experimental values. The calculated heat of formation showed that the $CeCu_2$-YCu_2 and YZn_2 Laves phase was of the strongest alloying ability and structural stability. The electronic density of states (DOS) and charge density distribution were given.

1. INTRODUCTION

This paper concentrates on a particular class of intermetallic phases, the so-called Laves phases. These phases, which form the largest group of intermetallic with more than 1400 representatives, have the ideal composition AB_2. An intermetallic compound is classified as a Laves phase purely on the basis of the geometry of the crystal structure. The Laves phases crystallize in three structure types: cubic $MgCu_2$ *(C15)*, hexagonal $MgZn_2$ *(C14)* and hexagonal $MgNi_2$*(C36)* [1–4]. An orthorhombic structure also exists where are observed a number of AB_2 intermetallics, namely the $CeCu_2$-type structure.

In the past decades several heuristic approaches to describe the stability have been applied to the family of Laves phases. In particular geometrical concepts relying on symmetry, packing density or electronic factors like valence electron concentration or the difference in electronegativity have been considered. However, these concepts are of limited value. They have turned out to be of low predictability even in binary systems and they are inapplicable for extrapolation, e.g., by introducing more components.

The exploration of Laves phases as materials components has revealed many problems in our understanding of intermetallics. A break-through in the targeted development of materials with superior properties based on intermetallics compared to steel alloys can only be expected after a much better understanding of their stability and chemical bonding [5]. First-principles density functional theory calculations have been broadly used to study the electronic structure and mechanical properties of laves phase compound. Two groups have used the linear muffin-tin orbital (LMTO-NFP) to study these compounds. B. Mayer *et al.* [6] studied the MAl_2 (M=Ca, Y, Sc and La) and MCr_2 (M=Ti, Zr, Nb and Ta), K.S. Kumar *et al.* [7,8] studied theMCr_2 (M=Ti, Zr, Ta, Nb, Sc, Y, La), other three groups have used the Vanderbilt-type ultrasoftpseudopotentiel (USPP) incorporated in the Vienna ab initio simulation package (VASP), Xiaoma Tao *et al.* [9] studied MAl_2 (M = Sc, Y, La, Ce–Lu), Yifang Ouyang *et al.* [10] studied the MMg_2 (M=La, Ce, Pr, Nd, Pm, Sm, Gd), Subhadeep Kal *et al.* [11] studied the MZn_2 (M=Ca and Sr) and MAl_2 (M=Sr and Ba); Their results showed that density functional theory (DFT) calculations can give satisfactory values that would often be otherwise difficult to obtain directly from experiments. In this paper, we have performed ab initio calculations to investigate the stability, electronic and structural properties of YCu_2 and YZn_2.

2. CALCULATION METHODS AND CRYSTAL STRUCTURES

Calculations were performed using the VASP [12–14] code based on the density functional theory (DFT) [15,16]. Ultrasoft Vanderbilt-type pseudopotentials [17] were used to describe the interactions between ions and electrons. The generalized gradient approximation (GGAPW91) due to Perdew and Wang [18] was applied to evaluate the exchange-correlation energies of all examined structures. Sampling of the Brillouin zone was done via $9 \times 9 \times 9$ and $11 \times 11 \times 11$ k-point grid generated according to the Monkhorst–Pack scheme [19] for YCu_2 and YZn_2 respectively. The cut-off energy restricting the number of plane waves in the basis set was set to 292.2 eV for YCu_2 and 261.9 eV for YZn_2.

Laves phases belong to the class of Frank–Kasper phases showing topologically close-packed structures. They have the general composition AB_2 with the larger A atoms in the centre of a 16-atom Frank–Kasper polyhedron and the smaller B atoms in the centers of icosahedra. The coordination number for the A atoms is 16 (4A and 12B atoms) and 12 (6A and 6B atoms) for the B atoms. The closest packing of hard spheres of types A and B is obtained for the radius ratio $r_A/r_B = (3/2)^{1/2} \approx 1.225$ [20].

The structural relaxation and optimization have been performed from the above configurations. The energies of these AB_2 Laves phases were minimized to determine the internal atomic coordinates. The obtained optimal atomic coordinates from energy minimization were *Y 4f (0.33, 0.67, 0.062), Cu (Zn) 2a (0, 0, 0) and Cu (Zn) 6h (0.83,*

Table 1. The calculated ground state properties of pure elements. Experimental values are listed in parentheses, cell parameters (a, b, c in Å), bulk modulus (GPa).

Parameters/ metals	Y	Cu	Zn
Valence electrons	s^1d^2	$d^{10}p^1$	$d^{10}p^2$
Space group	*P6$_3$/mmc*	*Fm3m*	*P6$_3$/mmc*
Z	3	11	12
Cell angles	90/60	90	90/60
Cell constants			
a = b	3.63	3.64	
	(3.65)[a]	(3.61)[a]	(2.66)[a]
C	5.61	–	5.02
	(5.73)[a]	–	(4.95)[a]
Bulk modulus	58.42	139.3	123.28
	(58.56)[a]	(137.0)[a]	(95.68)[a]

[a]Ref. [24].

0.66, 0.25) sites for C14 Laves phase structure, and *Y 8a (0.125, 0.125, 0.125) and Cu (Zn) 16d (0.50, 0.50, 0.50)* sites for C15 Laves phase, and *Y 4e (0, 0, 0.093), Y 4f (0.33, 0.67, 0.16), Cu (Zn) 6g (0.50, 0.50, 0.50) and Cu (Zn) 6h (0.16, 0.33, 0.25)* sites for C36 Laves phase structure [21].

However, these compounds often pass through phase transformations, especially to and from the orthorhombic $CeCu_2$ structure and the optimal atomic coordinates for this structure were *Ce 4e (0, 0.25, 0.5377) and Cu 8h (0, 0.0510, 0.1648)* [22].

3. RESULTS AND DISCUSSIONS

3.1. Stability and structural properties

We performed these calculations to investigate structural competition between some Laves phase structures for the systems YCu_2 and YZn_2. As Laves phase structures we considered cubic $MgCu_2$ (C15), hexagonal $MgZn_2$ (C14) and hexagonal $MgNi_2$ (C36).

As shown in Table 1 the cell parameters of pure Cu and Zn are overestimated whereas, many previous calculations on transition metals clearly indicated that cell constants were usually underestimated with standard DFT method, even GGA is applied, and it is the same for the bulk modulus of the two elements. While the calculation of cell parameters and bulk modulus of pure Y are in good agreement with the experimental values.

The total energy as a function of the cell volume was fitted by Birch-Murnaghan equation of state [25]. Then the lattice constants of YCu_2 and YZn_2 Laves phases were calculated and listed in Table 1, together with the lattice constants of pure Y, Cu and Zn. It can be seen that the obtained results of the lattice parameters were close to the available other theoretical values, and the errors was not more than 0.1 Å.

Figure 1 summarizes the results in the form of total energy vs. volume curves. For the 6 valence electron system YZn_2 the cubic $MgCu_2$ structure is preferred over the hexagonal $MgNi_2$ and the hexagonal $MgZn_2$ structure, this is in disagreement with the result obtained by *S. Kal et al.* [26], while for the 4 valence electron system

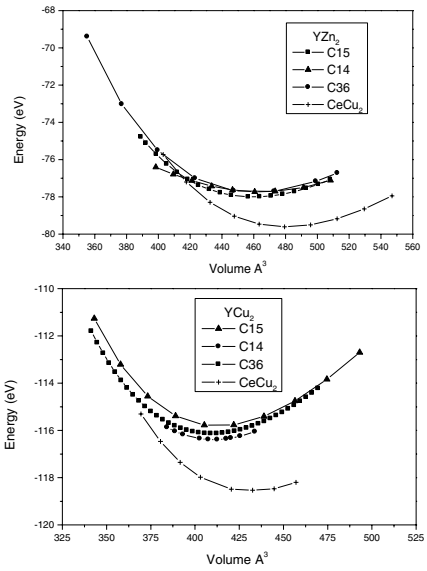

Figure 1. Total energy against volume for YCu_2 and YZn_2 in the C14, C15, C36 and $CeCu_2$ structures.

Table 2. Equilibrium values of the four units cells: the lattice constants (a, b, c in Å), bulk modulus (GPa) and their ratio *c/a* for the tow phases calculated with GGA, compared with experimental values listed in parentheses.

		YCu_2		YZn_2	
	Property	Theory	Exp. Ref.	Theory	Exp. Ref.
$CeCu_2$	a	4.3	(4.304)[b]	4.45	(4.504)[b]
Space	b	6.8	(6.863)[b]	7.12	(7.143)[b]
group	c	7.3	(7.291)[b]	7.57	7.664)[b]
imma	c/a	–	–	–	–
	B	85.643	–	72.414	–
C14	A	5.246	–	5.523	–
Space	c	8.609	–	8.776	–
group	c/a	1.641	–	1.588	–
P6$_3$/mmc	B	88.569	–	69.225	–
C15	a	7.432	–	7.717	–
Space	c	–	–	–	–
group	c/a	1.0	–	1.0	–
Fd-3m	B	87.193	–	47.577	–
C36	A	5.264	–	5.453	–
Space	c	17.183	–	17.894	–
group	c/a	3.264	–	3.281	–
P6$_3$/mmc	B	87.908	–	69.915	–

[b]Ref. [23].

YCu_2 the hexagonal $MgZn_2$ structure is preferred over the $MgNi_2$ and the cubic $MgCu_2$ structure.

Hexagonal and cubic Laves phases attain the same equilibrium volume for a particular system. The more open packed $CeCu_2$ structure yields a higher equilibrium volume (by about 5%) compared to the close-packed arrangements. This is similar with to the other theoretical and experiment results [27]. The stabilization of the $CeCu_2$ structure over a close-packed arrangement increases from YCu_2 and YZn_2.

For YCu_2 and YZn_2 the crossing of the energy-volume curves of the close-packed Laves phase structures and the orthorhombic $CeCu_2$ structure. From this behavior theory predicts a high-pressure structural transition.

Table 3. Pressure of transition (P_{tr} in GPa) from the $CeCu_2$ structure to Laves phase structures (C14, C15, C36) for YCu_2 and YZn_2 are presented.

	Pressure of transition P_{tr}		
	YCu_2		YZn_2
	Theory	[c] *Ref.*	
$CeCu_2$	–	–	–
C14	16.7	–	19.5
C36	17.5	–	14.8
C15	28.5	28	12.2

At 0 K (which the calculations refer to) $G = E + pV$. The difference in Gibbs-free energy G of two phases 1 and 2 at a given pressure p is given by the difference between intersections of parallel tangents $p = -(\partial E_1/\partial V)_{v=v1} = -(\partial E_2/\partial V)_{v=v2}$) with the ordinate axis. A transformation occurs at a pressure p_{tr} at which the tangents coincide ($\Delta G = 0$) [26]. With this so-called common tangent method transition pressures for a $CeCu_2$-type to Laves phase structural change are estimated as 16.7 GPa ($CeCu_2$ to C14) and 12.2 GPa ($CeCu_2$ to C15) for YCu_2 and YZn_2 respectively (show Table 3).

In summary, theory reproduces correctly the experimental ground state structures for YCu_2 and YZn_2 and predicts pressure-induced structural phase transitions from the $CeCu_2$-type to a Laves phase close-packing for the latter systems.

3.2. Enthalpy of formation

To investigate the alloying ability and stability, the formation energy (ΔE_f) of AB_2 type Laves phase were calculated by:

$$\Delta E_f = E_{tot}^{AB_2} - (E_{solid}^{A} + 2E_{solid}^{B}) \quad (1)$$

E_{solid}^{A} and E_{solid}^{B} represent the energy per atom of A and B in solid states.

At ambient conditions at the ground state (with temperature at zero Kelvin and pressure at zero bar), the enthalpy is equal to the energy, that is $\Delta E_f(AB_2) = \Delta H_f(AB_2)$ [28].

From Figure 2, we can see that for C14, C15, C36 and $CeCu_2$ structures the heat of formation for YCu_2(a) is −0.617, −0.546, −0.585, −0.884 eV/atom respectively, which are greater than −1.058, −1.137, −1.108, −1.188 eV/atom for YZn_2(b). From the values of the heat of formation in each AB_2 type binary Laves phase, we can see that the lowest heat of formation for YCu_2 and YZn_2 is of $CeCu_2$ structure, corresponding to the relatively stronger alloying ability of $CeCu_2$-YCu_2, $CeCu_2$-YZn_2 in each binary Laves phase, respectively.

3.3. Electronic structure

3.3.1. Densities of States

Electronic densities of state (DOS) and electron charge densities distributions were calculated to have a further

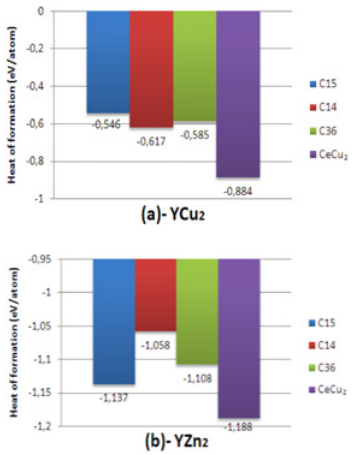

Figure 2. Heat of formation of (a)-YCu_2 and (b)-YZn_2.

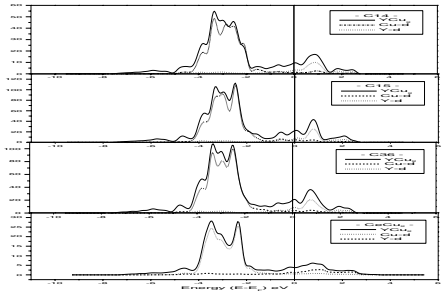

Figure 3. Calculated total DOS for YCu_2 Laves phase with C14, C15, C36 and $CeCu_2$ structures, along with the DOS of the constituent Y-d and Cu-d.

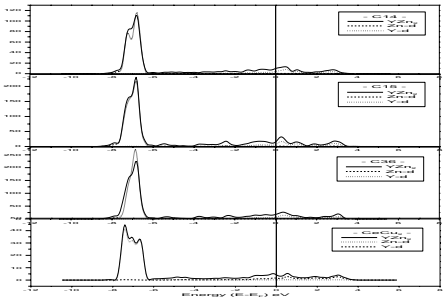

Figure 4. Calculated total DOS for YZn_2 Laves phase with C14, C15 and C36 structures, along with the DOS of the constituent Y-d and Cu-d.

insight into the bonding of YCu_2 and YZn_2 and then to reveal the underlying structural stability mechanism of these Laves phases.

Total and partial DOS of YCu_2 and YZn_2 are presented in Figure 3 and Figure 4.

As shown in Figure 3, the Cu-DOS plays a dominant and most important role in the total DOS of YCu_2. In the YCu_2- C14- C15- C36- $CeCu_2$ the Cu-DOS is mainly localized from about −5 to −1 eV. The same for the Y-DOS how have an important role in the Dos of YCu_2, in the YCu_2- C14- C15- C36 the Y-DOS is mainly localized from about −1 to 2.75 eV [29,30]. In Figure 6, we can see that the Zn-DOS have an important role in the DOS of YZn_2. In the YZn_2- C14- C15- C36 the Zn-DOS is mainly localized from about −8 to −6 eV, the same for the Y-DOS

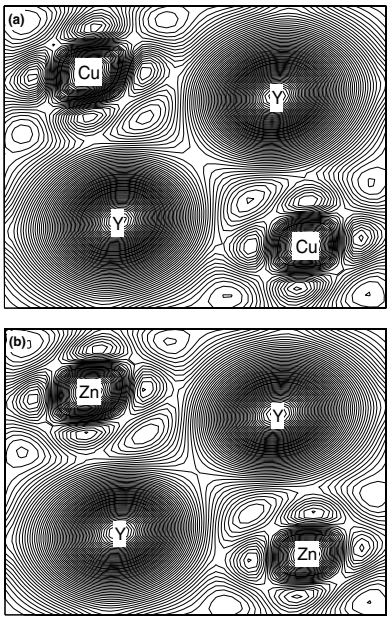

Figure 5. The contour plots of charge densities (a) The (0 1 0) plan for $CeCu_2$-YCu_2, (b) The (0 1 0) plan for $CeCu_2$ – YZn_2.

how is localized from −2 to 4 eV. And in the Fermi level we can see that the material have a metallic character in the tow intermetallics materials YCu_2- YZn_2 caused by the distribution of the electrons of the Y atoms (Figure 4).

3.3.2. Charge densities distribution

The charge-densities contour mapsof $CeCu_2$-YCu_2 (a), $CeCu_2$-YZn_2(b) in (010) and (010) planes respectively, and C14-YCu_2(c), C15-YZn_2(d) in (1 0 0) and (0 1 0) planes respectively are presented in Figure 5.

Higher density region corresponds to the core electron distribution of Cu and Y atoms that contributes relatively little to the bonding. In Figure 5(a), Y atoms are almost spherical, but Cu atoms are a little deformed. The obvious overlap of electron densities between Cu and Cu indicates a covalent bonding between them. In contrast to the Cu-Cu bonding, there is no overlap of electron densities around Y atoms. The almost uniform electron distribution around Y atoms exhibits a metallic bonding between Y and Y and can be well described by the nearly free electron model. The charge density distribution maps exhibit mainly an ionic bonding between Cu and Y atoms, which is a common feature for the electronic structure of AB_2 type Laves phases. In Figure 5(b), the charge density distribution indicates that there is covalent bonding between Zn and Zn, ionic bonding between Y and Zn and metallic bonding between Y and Y [31].

4. SUMMARY AND CONCLUSION

In conclusion, the calculated result of the heat of formation show that YZn_2 phase has the strongest alloying ability as well as the highest structural stability, next YCu_2. Our two composed have a high-pressure transition phase from the $CeCu_2$ structure to Laves phase structures, the boundary between open packed, polyanionic, $CeCu_2$ – type phases and close packed Laves phases is primarily governed by the electronegativity difference between the A and B component. The application of pressure has the effect of decreasing the electronegativity difference between components in binary systems (Figure 5). Thus $CeCu_2$ – type polar intermetallics can be compressed into Laves phases.

The charge density distributions show that for YCu_2 and YZn_2 type Laves phase, there are metallic bonding between Y and Y, covalent bonding between Cu (Zn) and Cu (Zn), while between the Y and Cu (Zn) atoms, and this is consistent with the difference in electronegativity between Cu (Zn) and Y atoms. This charge accumulation is typically characteristic of a polar covalent bonding.

References

[1] X. Nie, S. Lu, K. Wang, T. Chen, C. Niu, Mater. Sci. Eng. A **85** (2009) 502.
[2] D. J. Thoma, K.A. Nibur, K. C. Chen, Mater Sci. Eng. A **329** (2002) 408.
[3] H. Xu, X. Nie, Y. Du, S. Lu, K. Wang, Philos. Mag. Lett. **8** (2009) 465.
[4] J. Chao, Acta Mater. **55** (2007) 1599.
[5] F. Stein, M. Palm, G. Sauthoff, Intermetallics **12** (2004) 713.
[6] B. Mayer, H. Anton, E. Bott, M. Methfessel, J. Sticht, J. Harris. Intermetallics **11** (2003) 23.
[7] K.S. Kumar, D.B. Miracle. Intermetallics. **2** (1994) 257.
[8] K.S. Kumar, L. Pang, J.A. Horton, C.T. Liu. Intermetallics **11** (2003) 677.
[9] X. Tao, Y. Ouyang, H. Liu, F. Zeng, Y. Feng, Y. Du, Z. Jin. Computational Materials Science **44** (2008) 392.
[10] Y. Ouyang, X. Tao, H. Chen, Y. Feng, Y. Du, Y. Liu. Computational Material Science **47** (2009) 297.
[11] S. Kal, E. Stoyanov, J. Belieres, T. L. Groy, R. Norrestam, U. Häussermann, Journal of Solid State Chemistry **181** (2008) 3016.
[12] G. Kresse, J. Furthmüller, Physical Review B **54** (1996) 11169.
[13] G. Kresse, J. Furthmüller, Computational Materials Science **6** (1996) 15.
[14] G. Kresse, D. Joubert, Physical Review B **59** (1999) 1758.
[15] P. Hohenberg, W. Kohn, Physical Review B **136** (1964) 864.
[16] W. Kohn, L.J. Sham, Physical Review A **140** (1965) 1133.
[17] D. Vanderbilt, Physical Review B **41** (1990) 7892.
[18] J.P. Perdew, J.A. Chevary, S.H. Vosko, K.A. Jackson, M.A. Pederson, D.J. Singh, C. Fiolhais, Physical Review B **46** (1992) 6671.
[19] H.J. Monkhorst, J.D. Pack, Physical Review B **13** (1976) 5188.
[20] Y. Kitano, M. Takata, Y. Komura. J. Microsc. **142** (1986) 181.

[21] W. Yu, N. Wang, X. Xiao, Solid State Sciences **11** (2009) 1400.
[22] Allen C. Larson and Don T. Cromer, Acta Cryst. **14** (1961) 73.
[23] M.L. Fornasini, A. Iandelli, F. Merlo, M. Pani, Intermetallics **8** (2000) 239.
[24] W. Yu, N. Wang, X. Xiao, B. Tang, L. Peng, W. Ding, Solid State Sciences **11** (2009) 1400.
[25] F. Birch, Physical Review. **71** (1947) 809.
[26] S. Kal, E. Stoyanov, J-P. Belieres, T. Groy, R. Norrestam, U. Häussermann, Journal of Solid State Chemistry **181** (2008) 3016.
[27] A. Lindbaum, J. Hafner, E. Gratz and S. Heathman, J. Phys.: Condensed. Matter **10** (1998) 2933.
[28] C.M. Fang, M.A. Van Huis, H.W. Zandbergen, Computational Materials Science. **51** (2012) 146.
[29] C.L. Fu, X. Wang, Y.Y. Ye, K.M. Ho, Intermetallics **7** (1999) 179.
[30] J. Nyle'n, F.J. Garcı'a, B.D. Mosel, R. Pöttgen, U. Haüssermann, Solid State Science. **6** (2004) 147.
[31] A. Ormeci, F. Chu, J.M. Wills, Phys. Rev. B **54** (1996) 12753.